

The role of anomalous resistivities in Plasma Focus discharges

Horacio Bruzzone

Abstract The existence of plasma microturbulence in Plasma Focus (PF) devices is a widely accepted fact within the PF community. This microturbulence must be generated as a final stage of microscopic instabilities, which could develop during certain phases of the plasma evolution. Among the candidate instabilities to occur in these devices, the lower hybrid drift instability is the one with better possibilities, because its triggering condition (electron drift velocity approaching ion thermal velocity) has reasonable chances to be fulfilled. The main effect of the development of this instability is the modification of the collision frequencies in the plasma, which adds an anomalous term to the plasma resistivity. The theory for evaluating this extra term exists, and has been already used in PF 1D numerical simulations and in Z-pinch calculations. The role of this anomalous resistivity in PF behaviour has been the subject of considerable speculations. In this work, a 1D MHD (magneto-hydrodynamics) calculation of the pinch stage in a PF device will be presented, including anomalous resistivity effects and their influence on electric fields and the discharge current are discussed.

Key words anomalous resistivity • pinches • plasma focus

Introduction

Within the Plasma Focus community, there is a common belief that the most of the properties of these devices, when considered as neutron generators are due to some phenomena which make the plasma in the focus turbulent. The line of reasoning is essentially as follows: turbulence should give rise to an anomalous resistivity in the plasma, which should spread the current distribution but also produce a large electric field, sufficient to generate electron and ion beams which would be responsible for the neutron generation. Experimentally, there is no doubt of the production of such beams in Plasma Focus devices; however, the mechanism of their generation has not been satisfactorily explained. Furthermore, all of the measurements performed for these beams show that they have a maximum at filling pressures lower than that of the maximum neutron production and it is difficult to explain the neutron yield in large devices in terms of measured ion beam yields.

Without any pretension of giving definite assessments on the nature of neutron generation, the purpose of this work is to analyse the effect of anomalous resistivities in the focus stage of Plasma Focus devices. This will be done using a 1D MHD model, described later on, which includes the possibility of the appearance of an anomalous plasma resistivity originated in the later stages of the development of a lower hybrid drift instability (LHI). This type of anomalous resistivity has been selected for a number of reasons: it has the lower threshold condition, it is likely to exist in Plasma Focus (PF) plasmas [3] and, last but not least, is the

H. Bruzzone
ADEP, Facultad de Ciencias Exactas y Naturales,
Universidad de Mar del Plata y Pladema,
Funes 3350, 7600 Mar del Plata, Argentina,
Tel.: + 54223/ 4752426 ext. 457, Fax: +54223/ 4753150,
e-mail: bruzzone@mdp.edu.ar

Received: 23 October 2000, Accepted: 16 February 2001

only one (to my knowledge) which has a theory allowing the calculation of plasma resistivity.

LHI is triggered whenever the electron drift velocity v_d becomes comparable to or greater than the thermal ion velocity, v_i . This effect was discussed and carefully evaluated for theta-pinch plasmas [6], and later on used in the modelling of the pinch stage in a PF device [9] and in solid fibre Z-pinch plasmas [4, 8]. The feasibility of using the theory developed in the context of theta-pinch to Z-pinch plasmas was particularly discussed in the works by Chittenden [4, 5].

The main effect of LHI consists in the modification of the normal electron-ion collision frequency, ν_{ei} , through the addition of an anomalous collision frequency, ν^* , which is given by [8]:

$$(1) \quad \nu^* = 0.5 \sqrt{\frac{\pi}{2}} (\omega_{ce} \omega_{ci})^{1/2} \left(\frac{v_d}{v_i} \right)^2$$

where $\omega_{ce,i}$ are the electron and ion Larmor frequencies, respectively. As a consequence, the plasma resistivity η becomes, for deuterium plasma (MKS units are used):

$$(2) \quad \eta = \frac{m}{nc^2} (\nu_{ei} + \nu^*) = \eta_o + \eta_{an}$$

where m and e are the electron mass and charge, respectively, η_{an} is the anomalous resistivity and η_o is the standard Spitzer resistivity. An important feature of the anomalous term is that the dissipated (Joule) energy does not go only to the electrons, as usually, but also heats up the ions. Following Vikhrev and Braginskii [9], the Joule power per unit volume is assumed to be distributed as:

$$(3) \quad j^2 (0.13\eta + 0.87\eta_o) \text{ to electrons}$$

$$(4) \quad j^2 (0.87\eta - 0.87\eta_o) \text{ to ions}$$

where j is the current density.

The model

Similarly to work [9], the implosion of a plasma current sheet (CS) towards the axis of a PF device and the subsequent pinch formation will be calculated. The filling gas is deuterium, at a pressure p_o , and the model used in what follows is a 1D (radial), two temperatures (electron and ions) MHD Lagrangian numerical code derived from a 2D code developed by L. Bilbao [1]. It includes ion viscosity, ion and electron thermal conductivities and bremsstrahlung radiation, besides of the Joule heating described above.

The circuit equation (containing a capacitor with capacity C , charged at voltage V at the beginning of the CS implosion and a fixed inductance L , which includes the inductance of the gun) is:

$$(5) \quad \frac{d(L_i I)}{dt} = \frac{Q}{C} - h(\eta j)_{a(t)}; \quad Q = CV - \int_0^t I dt$$

where h is a fixed parameter, the assumed height of the imploding column and $a(t)$ is the plasma border and

$$(6) \quad L_i = L + \frac{\mu_o}{2\pi} h \ln \left(\frac{b}{a(t)} \right)$$

where b is the fixed external current return radius (the external electrode radius, say). It should be noted that (ηj) is the electric field in the plasma frame of reference.

The region under study is divided in a number NR of radial Lagrangian cells, having widths defined initially with the condition of equal mass in every cell. The initial particle density is assumed to be uniform and determined by the operating filling pressure of the device. This procedure improves the stability in the calculations, and also gives a better spatial resolution in the border zones, where an initial current density profile must be given to start the calculations.

Axial particle (mass) losses are also included. This is done to account for an essential feature in the plasma evolution that derives from the ‘‘conical’’ nature of the implosion and pinch stage. Conceptually, the plasma pressure in the converging plasma region of the whole CS bridging the electrodes is higher than that in the rest of the sheet, so that plasma movements along the sheet should exist. Following the ideas used by Vikhrev [9] and denoting by N the total particle content of a cell, the mass loss is evaluated for any cell as

$$(7) \quad \frac{dN}{dt} = -2 \frac{v_z}{h} N$$

where the ‘‘axial’’ velocity v_z is given by

$$(8) \quad \frac{dv_z}{dt} = 2 \frac{(p - p(0))}{h n m_i} - 2 \frac{v_z^2}{h}$$

and here p is the total plasma pressure (ions and electrons) in the given cell, $p(0)$ is its initial value and n is the plasma density and m_i is the ion mass. It should be noted that under these conditions, the particles content per unit length is always a diminishing function of time.

To perform a calculation, a set of parameters and initial conditions are needed, which should be selected on the basis of preliminary estimations, because one needs to start at the end of the run-down stage. The calculations that will be presented were done using the following set of parameters: $I(0) = 1.3$ MA, $V = 1$ kV, $C = 1250$ μ F, $L = 50$ nH, $b = 12$ cm, $h = 2$ cm, $a(0) = 4$ cm.

These parameters correspond roughly to the ‘‘small’’ diameter, 1 MJ Frascati PF device, and have been selected because plasma density profiles of the CS and of the pinch are available [7] for comparison purposes. The initial conditions for the plasma parameters in the cells ($NR = 100$) were chosen as follows: $n = 2.2 \times 10^{17}$ cm^{-3} (≈ 3 Torr) and electron and ion temperatures, $T_e = T_i = 2$ eV in all the cells.

The condition for starting a CS at the outer radius was done choosing a linear current density profile in the outer 10 cells (initially extending for ≈ 2 mm), with the peak at the border and with values consistent with the initial external current. The plasma velocity is zero everywhere, except in the outer 10 cells where small initial values (-5×10^5 cm/s) were assumed. As it will be shown, these initial conditions produce, after a relatively short transient, a converging CS similar to that observed in actual devices.

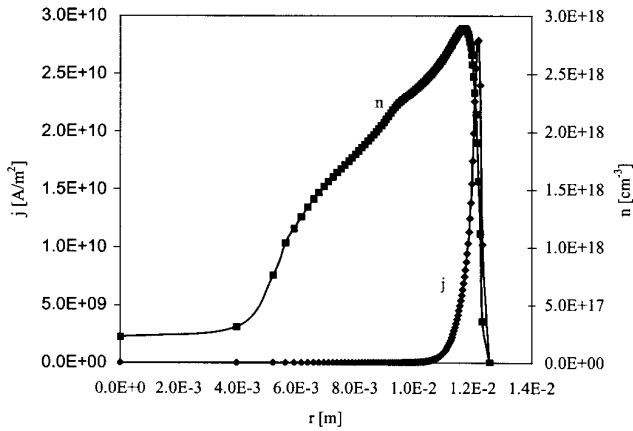


Fig. 1. n and j profiles in the CS at 155 ns.

It is well known that the plasma column formed in PF (and similar) devices suffer from macroscopic MHD instabilities, mainly of the $m = 0$ type. In particular, one should expect to find these instabilities developing in a PF column at the end of the first expansion, which follows the pinch formation. This situation is characterised by the largest value of inward radial acceleration, so that Rayleigh Taylor instabilities have the largest growth rate at this time. 1D codes cannot by themselves reproduce such a behaviour, but it can be incorporated into the code presented here by changing the value of h to a smaller one, h' (the assumed height of the micropinch) at the end of the first expansion. Consistently, the inductance of the rest of the pinch column (which is assumed to remain stationary) must be added to the external fixed inductance in the circuit equation.

Other physical effects essentially affecting the calculations will be incorporated into the code and discussed when appropriate.

Results

The code was run in a first version without including the option of describing the $m = 0$ instability. After a transient stage, which lasts less than 50 ns, a CS structure forms, with parameters substantially independent of the initial conditions. As an example, in Fig. 1, the current and plasma den-

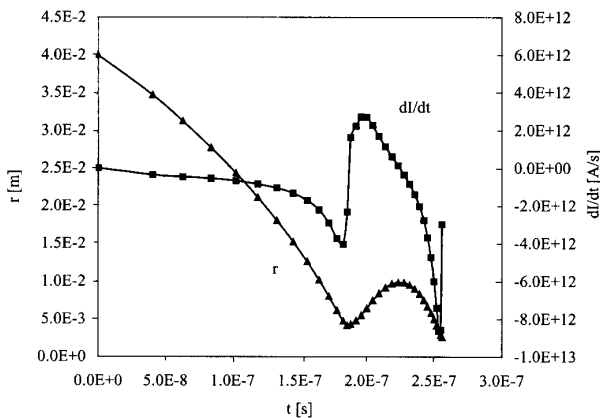


Fig. 3. Plasma external radius and dI/dt as a function of time.

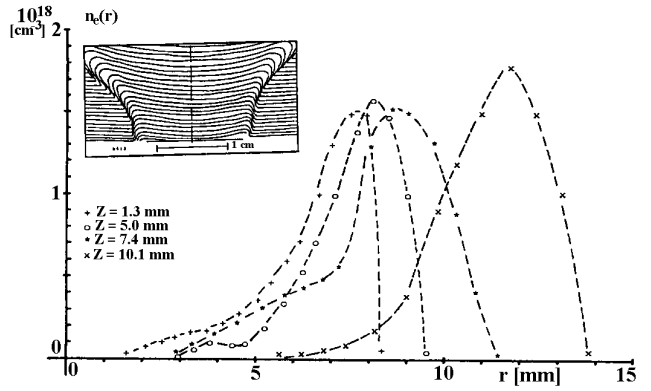


Fig. 2. Measured plasma density profiles of the imploding CS in the Frascati 1 MJ device [7], at different heights.

sities obtained at 156 ns are shown. The CS has reached a radial position of ≈ 1.2 cm, with a peak plasma density of $\approx 2.9 \times 10^{18} \text{ cm}^{-3}$, and a width of ≈ 6 mm. The current density distribution is concentrated in ≈ 2 mm, but occupies a number of cells more than double the initially used. Hence, the current density has diffused into the plasma, and its width is not determined by the initial choice of distribution. Note that the peak of current density is not on the border. This is due to the anomalous resistivity term, which is already larger than the standard one at the border.

For comparison purposes, measured plasma density profiles of the CS at different heights in the Frascati 1 MJ PF device [7] are given in Fig. 2. Peak values are by 50% smaller than those from the code but otherwise the agreement is rather good. Changing the initial value of the discharge current modifies the peak density values obtained from the code without significant changes in their profiles, so that it is possible to get closer agreement with the experimental curves if desired.

Comparison of the calculated plasma density profiles with the measured ones in later stages (column formation and evolution) also yield reasonable agreements. Some features of the overall behaviour of the results of the code are given in Figs. 3 and 4. Fig. 3 shows the evolution of the external plasma radius, r and of dI/dt as a function of time, up to ≈ 260 ns.

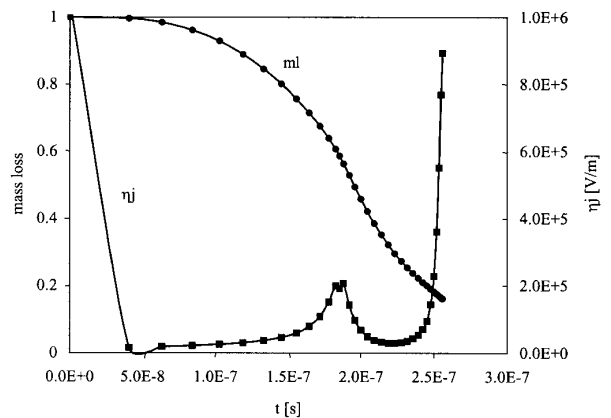


Fig. 4. Electric field (η_j) and fraction of the initial mass, m_l in the pinch vs. time.

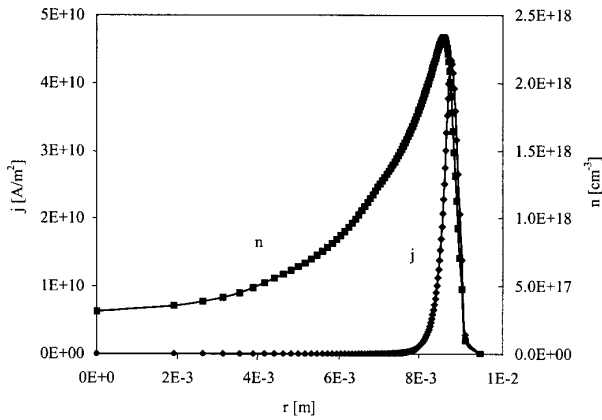


Fig. 5. n and j profiles at the end of the first expansion, $t = 223$ ns.

It can be seen that the plasma column attains a minimum radius of ≈ 4 mm at 188 ns and expands for a radius of ≈ 9 mm 35 ns later, after which a second compression starts. If the code is kept running in these conditions, a succession of compressions and expansions are seen, with smaller and smaller radius values, in time scales in the order of tens of ns. Instead of analysing this behaviour, it is assumed that at the end of the first expansion, a 2 mm height micropinch is developing.

In Fig. 4, the electric field (η_j) at the border of the plasma and the fraction of mass remaining in the plasma relative to the total mass content in the initial volume are given as functions of time. It can be seen that less than 30% of the swept mass remains in the pinch at the time of the first expansion, in reasonable agreement with the experimental result [7]. It can also be seen that the electric field on the border of the plasma is relatively small (< 2 kV/cm) up to the second compression, except the (artificially) high initial value, which is due to the low initial electron temperature value. Hence, this electric field (which includes the effect of the anomalous resistivity) cannot be responsible neither for the shape of dI/dt nor for particle accelerations.

As mentioned before, at the end of the first expansion, the code is switched to describe a possible $m = 0$ instability with a height set at $h' = 2$ mm, a reasonable value derived from the experiments. The current and plasma densities at this time are given in Fig. 5. Note that j has not diffused noticeably into the plasma. Ion temperatures are nearly constant at ≈ 560 eV, while electron temperatures are lower, varying from 260 eV on the border down to ≈ 6 eV in the centre of the pinch. The plasma is already under compression, but with small velocities of $\approx -6 \times 10^6$ cm/s.

The ensuing evolution of the micro pinch is quite different from that of the complete column. This arises essentially from the fact that now the mass loss is enhanced by the diminution of h (see the definition of v_z). In Fig. 6, n and j profiles in the micropinch are given at $t \approx 246$ ns, that is 13 ns after the change of h by h' . It can be seen that the external radius is now ≈ 2.5 mm, and that j has diffused somewhat in the plasma. In fact, almost 1/3 of the cells have anomalous resistivity values, with that in the border having $\eta \approx 3 \times 10^4 \eta_0$. At this instant of time, the ion temperatures are near 8 keV, the electron temperatures vary from 2 keV

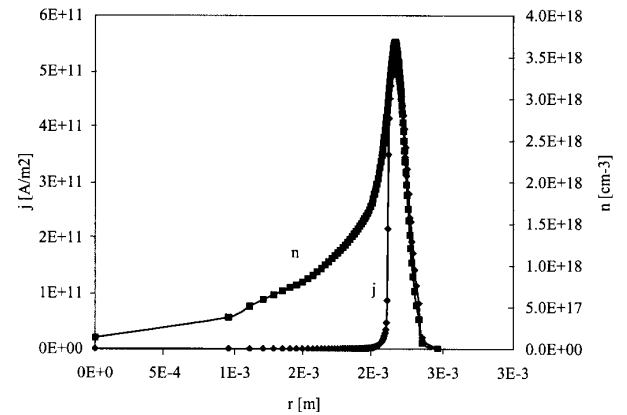


Fig. 6. n and j profiles in the micropinch at 246 ns.

on the border down to 380 eV in the centre, and the plasma is under compression with velocities $\approx -10^8$ cm/s.

The plasma evolution becomes now extremely fast. In Fig. 7 similar profiles are given 1 ns later on.

Now the plasma radius is ≈ 0.5 mm; the plasma is expanding with velocities of 7×10^7 cm/s, ion temperatures vary from 130 keV in the centre to 40 keV in the middle of the structure (due to shock heating) and rise again on the border up to 200 keV (due to anomalous Joule heating). Electron temperatures are smaller, varying between 3 keV in the centre up to 20 keV in the border. The values of the electric field on the border region are now much larger than in the column; at this moment they reach $\approx 10^8$ V/m.

An important feature to notice is the large diminution of n and j in the external cells of the structure. This diminution happens in such a way that the plasma pressure gradient overcomes the magnetic pressure one in this region, and the cells become relatively widened. If the calculations are continued one finds that the external radius of the pinch expands at a very large rate, but also that the external cells become so enlarged that its widths are no longer small when compared with their radial positions. Then, the evaluation of derivatives in this region yields wrong results. This numerical problem cannot be avoided by increasing the initial number of cells in the calculation. On the contrary, with a finer cell mesh, this problem simply appears at earlier times in the evolution.

The only way out of this situation is to check continuously the width of the external cell, and divide this cell in two with half widths, equal masses and the same intensive properties (density, temperatures, etc.) when its width exceeds a fixed fraction of the radius.

When this is done, another problem arises. The new cells keep expanding, having lower and lower densities and becoming more anomalous in resistivity. This indicates that an ablation phenomenon of the micropinch outer layer is in operation. However, at some moment, one finds that the magnetic diffusion velocity in the cells becomes comparable to (or larger than) the speed of light. This means that the displacement current cannot be neglected in the external cells, and a more elaborated calculation is required. An

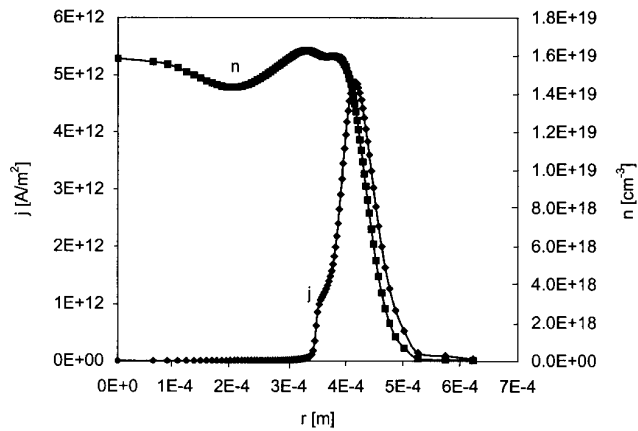


Fig. 7. n and j profiles in the micropinch at $t \approx 247$ ns.

intermediate approach based on throwing away the external cell when the magnetic diffusion velocity reaches a given fraction of the speed of light failed to solve the problem, because very rapidly the total number of the remaining cells became too small (less than 10), violating the requirements of the numerical procedure.

Conclusions

The 1D MHD code including anomalous resistivity and axial mass losses, developed for describing the implosion of a PF CS and the pinch formation has proven to be a useful tool for the study of these phenomena. The numerical results prove that, up to the stage of the development of an $m = 0$ instability, the role of the turbulence generated by LHI instabilities is only marginal in the gross plasma evolution. No important electric fields are generated, and very little current density diffusion exists. Admittedly, the model is rather crude and a 2D model would yield a better description of the problem, essentially because axial flows appear then in a natural way. However, such more complex (numerically) models do not include new physical phenomena, so that the results obtained with them should not differ essentially from those shown here. On this ground, the common belief existing in the PF community concerning the rel-

evance of turbulent phenomena in the focus stage is difficult to support.

The micropinch stage can be reasonably described during its initial phases. It is very fast and leads to an oscillating compression of the plasma down to a few hundreds of microns in radius, with very large temperatures. The later phases of this evolution cannot be described with the present code, because of the emergence of some physical problems strongly related to the anomalous resistivity. Whether the micropinch expand, as predicted by simpler 0D models [2], or tend to a rarefied plasma region (and end in some vacuum diode phenomena) is still an open question.

Acknowledgments This work was partially supported by grants from Mar del Plata University and the Agencia Nacional de Promoción Científica y Tecnológica, Argentina. Substantial parts of this work were possible thanks to the computational skills of L. Bernal.

References

1. Bernal L, Bilbao L (1998) Dynamics of a non-uniform hollow gas puff Z-pinch. *Il Nuovo Cimento D* 20:661–674
2. Bernal L, Bruzzone H, Bilbao L (1999) Anomalous resistivity in compressional Z-pinch. *J Tech Phys* 40:165–168
3. Bruzzone H, Bernal L (2001) Anomalous resistivities due to lower hybrid instabilities in plasma-magnetic field interfaces. *Nukleonika* 46;2 (in press)
4. Chittenden J (1994) Micro-turbulence in the fibre Z-pinch. In: 3rd Int Conf on Dense Z-pinch. AIP Conference Proceedings, vol. 299. AIP Press, New York pp 103–111
5. Chittenden J (1995) The effect of lower hybrid instabilities on plasma confinement in fiber Z pinches. *Phys Plasmas* 2:1242–1249
6. Davidson R, Krall N (1977) Anomalous transport in high-temperature plasmas with applications to solenoidal fusion systems. *Nucl Fusion* 17:1313–1372
7. Fischfeld G (1986) Estudio de propiedades de plasmas generados por medio de descargas eléctricas rápidas a través de técnicas diagnósticas ópticas. PhD Thesis. Universidad de Rosario, Argentine
8. Robson A (1991) Lower-hybrid-drift instability and radiative collapse of a dense Z-pinch. *Phys Fluids B* 3:1481–1486
9. Vikhrev V, Braginskii S (1986) Dynamics of the Z-pinch. In: Leontovich MA (ed) *Revs. Plasma Physics*. Consultants Bureau, New York 10:425–517